International Journal of Thermal Sciences 172 (2022) 107262

Contents lists available at ScienceDirect

International Journal of Thermal Sciences

journal homepage: www.elsevier.com/locate/ijts

Eigenfunction-based solution for one-dimensional solid-liquid phase change heat transfer problems with advection

Mohammad Parhizi, Ankur Jain *

Mechanical and Aerospace Engineering Department, University of Texas at Arlington, Arlington, TX, USA

ARTICLE INFO

Keywords:
Phase change heat transfer
Moving boundary problems
Analytical modeling
Melting
Solidification

ABSTRACT

Heat transfer problems involving solid-liquid phase change occur in a wide variety of engineering applications. Most phase change heat transfer problems do not admit an exact analytical solution, and therefore, development of approximate analytical methods is of much interest. This work analyzes a one-dimensional phase change heat transfer problem in the presence of advection due to fluid flow. An approximate, eigenfunction-based solution for the temperature distribution and propagation of the phase change front with time is derived, which may be interpreted as a generalization of the classical quasistationary method. It is shown that even a single term of this series offers improved accuracy compared to the classical quasistationary solution. The method is shown to retain good accuracy even at large values of the Stefan number where approximate analytical methods usually lose accuracy. Results are shown to be in good agreement with numerical simulation results. As expected, in the absence of advection, results are shown to reduce to well-known Neumann and Stefan solutions. The impact of various problem parameters, including Stefan and Peclet numbers on the rate of phase change front propagation is investigated. The theoretical treatment presented here can also be used to solve similar mass transfer problems with a chemical reaction front where species advection may play a key role. This work improves the theoretical understanding of phase change heat transfer in the presence of advection, and may find applications in the design and optimization of engineering processes and systems involving phase change.

1. Introduction

Melting and solidification are important heat transfer processes that occur in a large variety of scientific and engineering applications, including metallurgy [1], thermal management [2], energy storage [3] and desalination [4]. Mass transfer processes involving chemical reactions, such as growth of oxidation film [5] and the formation of Solid Electrolyte Interface (SEI) in a Li-ion cell [6] are also often mathematically described by similar equations. These heat and mass transfer processes are characterized by a moving phase change and reaction front, respectively. The foremost interest is often in determining how the phase change front evolves with time, and how various problem parameters influence the phase change front propagation [7]. Such moving boundary problems have been widely studied both experimentally and theoretically for several decades [7–10]. Despite the vast research literature available [11], development of mathematical models for such problems continues to be of much interest due to the practical relevance of such problems.

Phase change heat transfer problems are, in general, non-linear in nature [7]. Phase change in a semi-infinite one-dimensional body driven by an imposed temperature at one end is one of the simplest phase change heat transfer problems. Referring to the melting process as shown in Fig. 1, for a constant imposed temperature on the left boundary, a self-similarity based analytical solution exists. Stefan [12] showed that if the solid is initially at the melting temperature, the temperature field is a function of a self-similarity variable, $\eta = x/\sqrt{\alpha_L t}$ and the phase change front location is proportional to $\sqrt{\alpha_L t}$, where α_L is the thermal diffusivity of the liquid. Neumann derived a similar result for the more general case of an initially subcooled solid [13]. The ratio of sensible heat to latent heat, referred to as the Stefan number, *Ste* is an important non-dimensional parameter in phase change problems [7,9].

Unfortunately, most phase change heat transfer problems beyond the simplest Stefan and Neumann problems do not admit an exact analytical solution. Therefore, much research has been carried out to develop approximate analytical solutions as well as numerical simulation techniques. Approximate techniques often assume a certain form of temperature distribution in the newly formed phase, based on which, expressions are derived for the phase change front location as a function of time. For example, in the quasi-stationary technique, a steady-state

* Corresponding author. 500 W First St, Rm 211, Arlington, TX, 76019, USA.
E-mail address: jaina@uta.edu (A. Jain).

https://doi.org/10.1016/j.ijthermalsci.2021.107262
Received 14 May 2021; Received in revised form 29 July 2021; Accepted 31 August 2021
Available online 28 September 2021

Nomenclature

C	heat capacity ($Jkg^{-1}K^{-1}$)
ΔH_{LS}	latent heat of phase change (Jkg^{-1})
k	thermal conductivity ($Wm^{-1}K^{-1}$)
L	lengthscale (m)
Pe	Peclet number, $Pe = \frac{UL}{\alpha_L}$
Ste	Stefan number, $Ste = C_L(T_{ref} - T_m)/\Delta H_{LS}$
T	temperature (K)
V	flow velocity (ms^{-1})
x	spatial coordinate (m)
t	time (s)
α	diffusivity (m^2s^{-1})
β^2	ratio of thermal diffusivities, $\beta^2 = \frac{\alpha_L}{\alpha_S}$
γ^2	ratio of thermal conductivities, $\gamma^2 = \frac{k_L}{k_S}$
ρ	density (kgm^{-3})
τ	non-dimensional time, $\tau = \frac{\alpha_L t}{L^2}$
θ	non-dimensional temperature, $\theta_i = \frac{T_i - T_m}{T_{ref} - T_m}$, $i = L, S$
ξ	non-dimensional spatial coordinate, $\xi = \frac{x}{L}$
λ	non-dimensional eigenvalue

Subscripts

in	initial temperature
L	liquid phase
LS	phase change front
m	phase change temperature
ref	reference
S	solid phase
0	imposed temperature

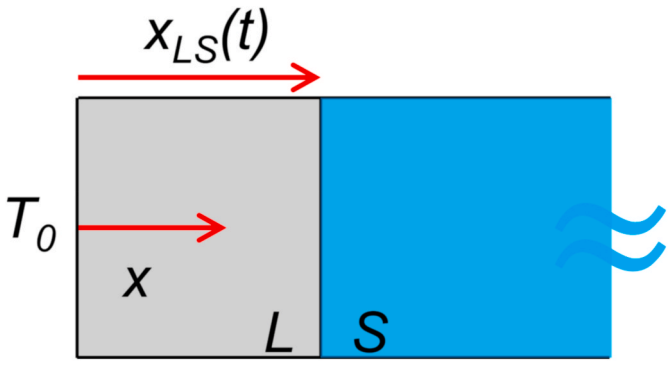

Fig. 1. Schematic of the geometry with diffusion and advection in a one-dimensional semi-infinite solid slab undergoing phase change to liquid due to an imposed temperature on the boundary and uniform fluid flow in the newly formed phase. The case of freezing of a liquid and mass transfer problems can be similarly analyzed.

temperature distribution is assumed by neglecting the transient term in the energy equation [7]. The resulting expression is valid only for small values of *Ste* [7]. Perturbation methods that express the temperature distribution as a power series expansion about *Ste* have also been used widely [14,15]. Such a solution is also valid only for small values of *Ste*. The integral method, based on assuming a polynomial temperature profile has also been used to develop approximate analytical solutions to heat transfer problems involving phase change [16]. In addition, a number of numerical techniques have also been developed for phase change processes, such as fixed grid, variable grid and front-fixing methods [17]. These methods can be categorized into three main types – enthalpy method (EM) [18], effective heat capacity method (EHCM) [19], and heat source term method (HSTM) [20,21]. In the enthalpy method, the primary dependent variable is the total enthalpy which is a combination of sensible and latent heat [22]. In effective heat capacity method, temperature is the primary dependent variable and an effective heat capacity, representing both sensible and latent heats, is used instead of the enthalpy [22]. In HSTM method, however, the enthalpy is divided into sensible and latent terms, resulting in a heat source term in the governing equation [22].

A wide variety of more complicated phase change problems of practical relevance beyond the simple Stefan/Neumann problems have also been analyzed, using analytical and numerical techniques, such as those listed above. A few examples include problems with time-dependent boundary conditions [14], multi-dimensional phase change [23], phase change in binary alloys [9], phase change with temperature-dependent thermal properties [24], phase change problems involving heat generation [25,26], phase change problems with multiple moving boundaries [27], embedded and encapsulated PCMs [28,29], and inverse Stefan problems [30,31].

While most phase change heat transfer problems are governed by thermal diffusion in the solid and liquid phases, advection-based transport due to fluid flow may also be relevant in some problems. Heat may be transported to/from the phase change front due to a flow field in the liquid phase. In addition, a flow field may also exist in a porous solid. Advection may also be important to consider in the analysis of mass transport problems involving a chemical reaction front in order to accurately predict the location of the reaction front. The Stefan problem with convection has been described by the Navier–Stokes equations with no-slip boundary conditions and has been formulated based on the enthalpy porosity method [32]. Weak solutions has been presented for both steady state and transient Stefan problem with convection [33–35]. Numerical investigation of a transient convective melting of a paraffin wax inside a closed region has been developed [36]. Recently, the Immersed Boundary Smooth Extension method has been used to solve the Stefan problem coupled with natural convection [37]. Solution for the Stefan problem with convection has been presented for two cases of a fixed convection velocity and a convection velocity governed by the Navier-Stokes equation [38]. Similarity solution has been derived for a one-phase Stefan problem with convection subject to Dirichlet, Neumann, Robin or radiative–convective boundary conditions. In this study, the velocity of the convective term of the was assumed to depend on temperature and time [39]. The solution of a non-classical moving boundary problem with convection subject to a generalized boundary condition has been developed using the Legendre wavelet Galerkin computational method [40]. Enthalpy-based lattice Boltzmann method was used to solve a melting problem with natural convention [41]. A solution for a problem with convection and temperature-dependent thermal conductivity has been presented [21]. A similar problem has been solved using reciprocal transformation [22]. Finite-element based numerical computation of a phase change problem with advection has also been presented [23].

Most of the literature on Stefan problems with advection cited above relies on numerically solving the phase change problem coupled with equations governing the flow field, such as the Navier-Stokes equation. In contrast, it may be of interest to derive analytical solutions for phase change problems with simplified advection, such as constant velocity. Even if such analytical solutions may be approximate, as is the case with most phase change problems, such solutions may help better understand the fundamentals of phase change in such systems, as well as the parametric dependence of the phase change process.

This paper derives an approximate eigenfunction-based solution for

a one-dimensional phase change heat transfer problem with advection in the liquid phase. The technique, presented here for melting of a semi-infinite solid can also be used for solidification problems, as well as equivalent mass transfer problems. Transient temperature distribution in the newly formed phase is written in the form of an eigenfunction-based infinite series. This is shown to result in an ordinary differential equation (ODE) for the phase change location as a function of time that accounts for both diffusion and advection. While such an eigenfunction-based approach has been used in the past for simpler phase change problems [42,43], it does not appear to have been used for solving diffusion-advection problems. It is shown that even a single term in the infinite series provides sufficient engineering accuracy for most problems, and that the resulting solution may be interpreted as a refinement of the quasistationary method, offering greater accuracy, particularly at large *Ste*. Results are found to be in excellent agreement with numerical simulations, as well as self-similarity solutions for special cases. Results discussed in this paper expand the fundamental understanding of phase change heat transfer problems, and may help develop tools for optimizing phase change in several important engineering applications, such as phase change in porous media.

2. Problem definition

Consider solid-to-liquid phase change heat transfer in a one-dimensional semi-infinite solid slab as shown schematically in Fig. 1. Prior to the start of the phase change process at $t = 0$, the slab is solid at a temperature $T_{in} \leq T_m$, where T_m is the melting temperature of the material. While this work is presented in the context of melting, the opposite process – solidification of a liquid into a solid – can also be analyzed using the same treatment. In the present work, phase change is driven by a constant temperature $T_0 > T_m$ maintained on the left face, due to which, the solid slowly melts into liquid, and the phase change front propagates towards the right. A uniform and constant fluid velocity U is assumed in the newly formed liquid phase. In the case of a porous solid, a fluid velocity may also exist in the solid phase, but is not considered here. It is of interest to determine the impact of heat transfer due to advection on the phase change process. As is common with phase change heat transfer processes, the primary interest is in determining the location of the phase change front as a function of time. Thermal conductivity, heat capacity, density and diffusivity are denoted as k, C, ρ and α, respectively, and subscripts L and S are used to denote the liquid and solid phases, respectively. The latent heat of phase change is denoted as ΔH_{LS}. Phase change is assumed to occur at a fixed temperature T_m. All properties are assumed to be independent of temperature. Natural convection in the liquid phase is neglected.

When the solid slab is initially at a subcooled temperature $T_{in} < T_m$, a temperature gradient exists in both solid and liquid phases. This is often referred to as the two-phase problem. As a special case, if $T_{in} = T_m$, i.e., the solid is initially at the melting temperature, heat transfer occurs only in the liquid phase and there is no temperature gradient in the solid. This problem is often referred to as the one-phase problem. In the absence of advection, the one-phase and two-phase problem have exact solutions, derived first by Stefan [12] and Neumann [13], respectively. A self-similarity-based solution, however, is not expected to exist in the presence of advection.

3. Derivation of solution for two-phase heat transfer problem with advection

Under the assumptions listed above, the governing energy conservation equations for the solid and liquid phases are given by

$$\frac{\partial^2 T_L}{\partial x^2} - \frac{V}{\alpha_L}\frac{\partial T_L}{\partial x} = \frac{1}{\alpha_L}\frac{\partial T_L}{\partial t} \tag{1}$$

$$\frac{\partial^2 T_S}{\partial x^2} = \frac{1}{\alpha_S}\frac{\partial T_S}{\partial t} \tag{2}$$

where the second term in equation (1) represents advection in the liquid phase due to an imposed uniform flow velocity V. Heat transfer in the solid phase is assumed to occur only due to diffusion. When considering a porous solid, the treatment presented here can be easily extended to account for advection due to fluid flow through the porous solid. Boundary conditions associated with equations (1) and (2) are

$$T_L = T_0 \; at \; x = 0 \tag{3}$$

$$T_L = T_S = T_m \; at \; x = x_{LS}(t) \tag{4}$$

$$T_S = T_{in} \; as \; x \to \infty \tag{5}$$

In addition, conservation of energy at the interface requires that net heat flow into the interface be balanced by the rate of heat consumption due to phase change at the interface [7], i.e.,

$$-k_L\left[\frac{\partial T_L}{\partial x}\right]_{x=x_{LS}} + k_S\left[\frac{\partial T_S}{\partial x}\right]_{x=x_{LS}} = \rho_L \Delta H_{LS}\frac{dx_{LS}}{dt} \tag{6}$$

The initial condition is

$$T_S = T_{in} \; at \; t = 0 \tag{7}$$

This problem is first non-dimensionalized to ensure generality of the solution. The following non-dimensional variables are introduced: $\theta_L = \frac{T_L - T_m}{T_{ref} - T_m}$, $\theta_S = \frac{T_S - T_m}{T_{ref} - T_m}$ $\xi = \frac{x}{L}$, $\tau = \frac{\alpha_L t}{L^2}$, where L is an arbitrary reference length, and T_{ref} is a reference temperature, which is taken to be equal to T_0 in this work. This results in the following set of non-dimensional equations

$$\frac{\partial^2 \theta_L}{\partial \xi^2} - Pe\frac{\partial \theta_L}{\partial \xi} = \frac{\partial \theta_L}{\partial \tau} \tag{8}$$

$$\frac{\partial^2 \theta_S}{\partial \xi^2} = \beta^2 \frac{\partial \theta_S}{\partial \tau} \tag{9}$$

where $Pe = \frac{VL}{\alpha_L}$ is the Peclet number that represents the ratio of advection and diffusion. $\beta^2 = \frac{\alpha_L}{\alpha_S}$ is the ratio of thermal diffusivities.

The non-dimensional boundary conditions are

$$\theta_L = 1 \; at \; \xi = 0 \tag{10}$$

$$\theta_L = \theta_S = 0 \; at \; \xi = \xi_{LS}(\tau) \tag{11}$$

$$\theta_S = \theta_{in} \; as \; \xi \to \infty \tag{12}$$

where $\theta_{in} = \frac{T_{in} - T_m}{T_{ref} - T_m}$. Note that by definition, θ_{in} is negative since the solid is initially subcooled below melting temperature. Also, $\xi_{LS} = \frac{x_{LS}}{L}$ is the non-dimensional location of the phase change front, which is a quantity of much practical interest.

The non-dimensional initial condition is

$$\theta_S = \theta_{in} \; at \; t = 0 \tag{13}$$

Finally, the non-dimensional equation representing conservation of energy at the interface is given by

$$-\left[\frac{\partial \theta_L}{\partial \xi}\right]_{\xi=\xi_{LS}} + \frac{1}{\gamma^2}\left[\frac{\partial \theta_S}{\partial \xi}\right]_{\xi=\xi_{LS}} = \frac{1}{Ste}\frac{d\xi_{LS}}{d\tau} \tag{14}$$

where $Ste = \frac{C_L(T_{ref} - T_m)}{\Delta H_{LS}}$ is the Stefan number and $\gamma^2 = \frac{k_L}{k_S}$ is the ratio of thermal conductivities.

In the absence of advection, i.e. $Pe = 0$, the problem defined above is the standard Neumann problem, which admits a self-similarity solution [7]. In this work, this problem is solved in the presence of advection. The most general problem of an initially subcooled solid, resulting in heat

transfer in both phases, is considered first. Results for the special case of the solid initially at T_m is easily obtained from the general solution. The general methodology followed here is to treat the heat transfer problem in the liquid as a transient problem in a wall of thickness ξ_{LS}, followed by the use of energy conservation at the interface, equation (14) to derive an ordinary differential equation for ξ_{LS} as a function of time.

The solid phase problem is considered first. Since no advection is considered in the solid, this is a problem of thermal diffusion into a semi-infinite body. A self-similarity based solution of equation (9) subject to boundary and initial conditions given by equations (11)–(13) can be written as follows [17]

$$\theta_S(\xi,\tau)=\theta_{in}\left[\frac{erf\left(\frac{\beta\xi}{2\sqrt{\tau}}\right)-erf\left(\frac{\beta\xi_{LS}}{2\sqrt{\tau}}\right)}{1-erf\left(\frac{\beta\xi_{LS}}{2\sqrt{\tau}}\right)}\right] \tag{15}$$

On the other hand, the liquid phase problem does not admit a self-similarity based solution due to the finite size of the liquid domain as well as the presence of advection. While the advective term can be removed through an appropriate transformation [17] to lead to a pure-diffusion equation, doing so results in time-dependent terms in the boundary conditions, which also rules out a self-similarity based solution. Instead, the method of separation of variables is used to derive a solution of the liquid phase problem, particularly equation (8), along with a zero temperature initial condition. This represents a problem of transient diffusion from a high temperature boundary into a one-dimensional body of fixed size ξ_{LS}. This is in contrast with the quasi-stationary method, which completely ignores the transient term and effectively considers only the steady-state portion of the transient temperature distribution derived here. Since the phase change front itself is dynamic, this technique is not expected to result in an exact solution. However, for pure-diffusion problems, this method has been shown to be more accurate than the quasistationary technique [43]. The accuracy of this technique in the presence of advection and limits on its validity is investigated in Section 4.

Since one of the boundary conditions associated with equation (8) is non-homogeneous, the solution is split into two parts as follows [17].

$$\theta_L(\xi,\tau)=w(\xi,\tau)+s(\xi) \tag{16}$$

where $s(\xi)$ accounts for the non-homogeneity in the boundary condition, and $w(\xi,\tau)$ can be used to solve the remainder of problem. A solution for $s(\xi)$ may be written as

$$s(\xi)=\frac{exp(Pe\xi)-exp(Pe\xi_{LS})}{1-exp(Pe\xi_{LS})} \tag{17}$$

On the other hand, $w(\xi,\tau)$ satisfies the following convection-diffusion equation

$$\frac{\partial^2 w}{\partial\xi^2}-Pe\frac{\partial w}{\partial\xi}=\frac{\partial w}{\partial\tau} \tag{18}$$

$w(\xi,\tau)$ must satisfy homogeneous boundary conditions. A solution for equation (18) can be written as follows [17]:

$$w(\xi,\tau)=\sum_{n=1}^{\infty}A_n\sin(\omega_n\xi)\exp\left(Pe\frac{\xi}{2}-\lambda_n^2\tau\right) \tag{19}$$

where only the sine eigenfunction is considered due to the nature of the boundary conditions. Further, the eigenvalue ω_n is given by $\omega_n=\frac{n\pi}{\xi_{LS}}$ due to the homogeneous boundary conditions. Finally, substituting equation (19) in the governing equation for $w(\xi,\tau)$, given by equation (18) results in the following relationship between λ_n and ω_n:

$$\lambda_n^2=\omega_n^2+\frac{Pe^2}{4} \tag{20}$$

Finally, the unknown coefficients A_n are determined using the initial condition and the principle of orthogonality of eigenfunctions. This results in

$$A_n=\frac{\int_0^{\xi_{LS}}-s(\xi^*)exp\left(-Pe\frac{\xi^*}{2}\right)\sin(\omega_n\xi^*)d\xi^*}{\int_0^{\xi_{LS}}\sin^2(\omega_n\xi^*)d\xi^*} \tag{21}$$

This completes the solution for temperature distribution in the liquid phase, given by equation (16). Note that the phase change location $\xi_{LS}(\tau)$ that appears in the solid and liquid phase temperature distributions is yet unknown. $\xi_{LS}(\tau)$ is usually the quantity of most practical interest, as it represents the propagation of the phase change front over time. In order to determine $\xi_{LS}(\tau)$, equations (15) and (16) are substituted into equation (14) that represents conservation of energy at the interface. With some mathematical simplification, this results in the following ordinary differential equation for $\xi_{LS}(\tau)$

$$\frac{d\xi_{LS}}{d\tau}=-Ste\left[Pe\frac{exp(Pe\xi_{LS})}{1-exp(Pe\xi_{LS})}+\sum_{n=1}^{\infty}\left[A_n\frac{n\pi}{\xi_{LS}}\cos(n\pi)\exp\left(Pe\frac{\xi_{LS}}{2}-\lambda_n^2\tau\right)\right]-\frac{\theta_{in}}{\gamma^2}\frac{\beta}{\sqrt{\pi\tau}}\frac{exp\left(-\left(\frac{\beta\xi_{LS}}{2\sqrt{\tau}}\right)^2\right)}{1-erf\left(\frac{\beta\xi_{LS}}{2\sqrt{\tau}}\right)}\right] \tag{22}$$

An initial condition for equation (22) is simply that $\xi_{LS}=0$ at $\tau=0$. Equation (22) is a complicated non-linear ordinary differential equation, from which, determining an expression for $\xi_{LS}(\tau)$ may be difficult. However, equation (22) provides an explicit expression for $\frac{d\xi_{LS}}{d\tau}$, and therefore, $\xi_{LS}(\tau)$ can be easily obtained by straightforward numerical integration. Numerical integration of an explicit ordinary differential equation such as equation (22) can be carried out using several available algorithms with high accuracy and speed, and is not expected to contribute significantly to error for this method.

This completes the derivation of the solution for both the phase change propagation front as well as the temperature distribution. Note that the first term on the left-hand side represents the well-known quasi-stationary solution that accounts for advection, whereas the infinite series in the second term may be interpreted as a correction factor that is shown in Section 4 to improve the accuracy of the method. Accordingly, the eigenfunction expansion based solution of the diffusion-advection problem is a generalization of the quasistationary technique, with improved accuracy.

A practical challenge related to this solution is encountered at the first timestep of the numerical integration, at which, $\xi_{LS}=0$, and therefore, $\frac{d\xi_{LS}}{d\tau}$ is infinite. This is because theoretically, the phase change process is infinitely fast at $\tau=0$ due to the sudden jump in temperature from $\theta=0$ to $\theta=1$ at the left face of the body, $\xi=0$. In order to overcome this difficulty, advection is ignored for the first timestep, and

the Neumann solution is used to determine the location of the phase change front at the end of the first timestep. Equation (22) is then used for all subsequent timesteps. Provided that the time step is reasonably small, this does not incur significant error.

Note that a key advantage of the present work is that $\xi_{LS}(\tau)$ – the quantity of interest in most applications – can be obtained directly from equation (22) without the need for computing the temperature distribution. In contrast, a typical numerical computation technique requires discretization of the entire geometry, followed by computation of the temperature at each node, which can be time-consuming. Further, as shown in the next Section, the solution presented here can be computed with only a few number of eigenvalues, which also contributes towards the advantage of this technique compared to numerical computation tools. For a typical Stefan problem with advection, it is found that the present technique computes $\xi_{LS}(\tau)$ in less than 1.0 s on a 2.80 GHz personal computer, compared to around 5.0 s for a finite-difference based numerical code on the same computer.

4. Results and discussion

4.1. Special cases

If the semi-infinite solid is initially at the melting temperature, no heat transfer will occur in the solid, and the problem reduces to a one-phase Stefan problem with advection. In this case, $\theta_{in} = 0$, and therefore, $\theta_s = 0$ at all ξ and τ. The phase change front in such a case is given by the following simplified equation

$$\frac{d\xi_{LS}}{d\tau} = -Ste\left[Pe\frac{exp(Pe\xi_{LS})}{1-exp(Pe\xi_{LS})}+\sum_{n=1}^{\infty}A_n\left[\frac{n\pi}{\xi_{LS}}\cos(n\pi)+\frac{Pe}{2}\sin(n\pi)\right]\exp\left(Pe\frac{\xi_{LS}}{2}-\lambda_n^2\tau\right)\right] \tag{23}$$

Further, for a pure diffusion problem, the following limits apply

$$\lim_{Pe\to 0}\frac{exp(Pe\xi)-exp(Pe\xi_{LS})}{1-exp(Pe\xi_{LS})} = 1-\frac{\xi}{\xi_{LS}} \tag{24}$$

and

$$\lim_{Pe\to 0}\frac{Pe\cdot exp(Pe\xi_{LS})}{1-exp(Pe\xi_{LS})} = -\frac{1}{\xi_{LS}} \tag{25}$$

Therefore, the phase change front for this special case is given by

$$\frac{d\xi_{LS}}{d\tau} = -Ste\left[-\frac{1}{\xi_{LS}}-\sum_{n=1}^{\infty}\left[\frac{2}{\xi_{LS}}\cos(n\pi)\exp\left(-\lambda_n^2\tau\right)\right]-\frac{\theta_{in}}{\gamma^2}\frac{\beta}{\sqrt{\pi\tau}}\frac{exp\left(-\left(\frac{\beta\xi_{LS}}{2\sqrt{\tau}}\right)^2\right)}{1-erf\left(\frac{\beta\xi_{LS}}{2\sqrt{\tau}}\right)}\right] \tag{26}$$

which is identical to the solution for the pure-diffusion Neumann problem derived using the separation of variables approach. While the exact solution for this problem is based on self-similarity [7], the solution obtained from equation (26) has reasonable accuracy, particularly for small *Ste*. The first term on the left-hand side represents the quasi-stationary solution, which, in the absence of advection, predicts a $\sqrt{t}$ dependence of the phase change front.

4.2. Verification

The eigenfunction-based solution presented in Sections 2 and 3 is compared against standard solutions for special cases for verification. In addition, results from the present work are also compared with a numerical simulation.

The special case of pure diffusion ($Pe = 0$) is considered first, in which, diffusion through the liquid phase drives the propagation of the phase change front. Self-similarity based exact solutions for this problem are available, for both one-phase [7,12] and two-phase [7,13] problems. Fig. 2(a) and (b) present a comparison of results from the present work with these exact solutions. The location of the phase change front is plotted as a function of time for four different values of *Ste* for a two-phase problem in Fig. 2(a). In addition, temperature distributions in both phases are plotted at three different times for a fixed value of $Ste = 0.24$ in Fig. 2(b). Non-dimensional problem parameters are $\theta_{in} = -1.5$, $\beta = 1, \gamma = 1$. In order to be able to compare with exact solutions, $Pe = 0$ is assumed for both Figures. Fig. 2(a) shows, as expected, rapid phase change front propagation at early times, followed by a slow down. The larger the value of *Ste*, which represents the temperature difference that drives the phase change process, the faster is the rate of propagation of the phase change front, as expected. In each case, there is good agreement between the present work and the exact solution. The agreement is

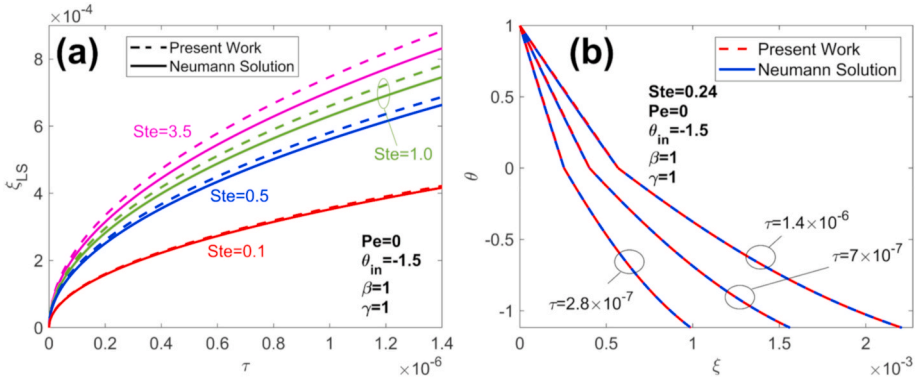

Fig. 2. Comparison of present work with self-similarity based Neumann solution for zero advection: (a) Phase change front ξ_{LS} as a function of τ for four different values of *Ste*; (b) Temperature distribution in both phases at three different times for a fixed value of *Ste*. Other problem parameters are $\theta_{in} = -1.5; \beta = 1; \gamma = 1$.

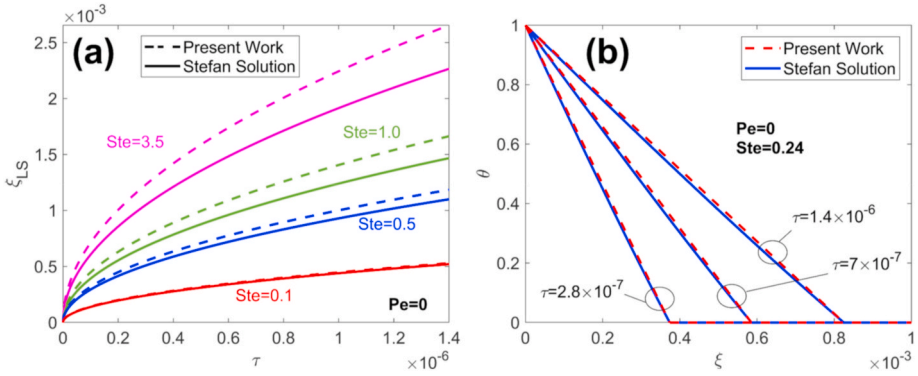

Fig. 3. Comparison of present work with self-similarity based Stefan solution for zero advection: (a) Phase change front ξ_{LS} as a function of τ for three different values of *Ste*; (b) Temperature distribution in liquid phases at three different times for a fixed value of *Ste*.

not exact because of the approximation involved in the present work by modeling the heat transfer problem in the liquid with a transient thermal model for a body of fixed size. Nevertheless, the agreement in Fig. 2(a) even for a reasonably high value of $Ste = 1.0$ is within 5%, which is quite low. The key source for this error is the approximation of treating the phase change interface to be constant at each time in deriving an eigenfunction-based solution for the temperature distribution. It is also shown later that unlike other approximate analytical methods, this method offers reasonable accuracy even at large *Ste*.

The temperature distribution plotted in Fig. 2(b) shows, as expected, a value of 1 at $\xi = 0$, and a value of 0 at $\xi = \xi_{LS}$ at each time. Since this is a two-phase problem, there is a temperature field in the solid phase as well, and the temperature curves are seen to approach the initial value of $\theta_{in} = -1.5$ at large values of ξ. There is excellent agreement between the temperature distributions predicted by the present model and the exact solution.

A similar comparison with the exact solution available for the one-phase Stefan problem without advection is presented in Fig. 3. Similar to Fig. 2(a), a $\sqrt{\tau}$ dependence of the phase change front location is seen in Fig. 3(a), with good agreement between the present work and the exact Stefan solution. There is also excellent agreement for the predicted temperature distributions at multiple times, as shown in Fig. 3(b) for $Ste = 0.24$. Note that since the original solid phase is initially at the melting temperature, there is no temperature field in the solid phase at any time during the phase change propagation process.

Based on Figs. 2 and 3, in order for the error to remain less than 10% for the zero advection case, an upper bound for *Ste* is found to be around 0.6 for the Stefan problem, whereas, for the Neumann problem, the error remains less than 10% even for very large *Ste*.

The comparisons presented in Figs. 2 and 3 are for the special case of zero advection, for which exact solutions are available. For further verification of the theoretical model presented in this work, comparison with a numerical simulation is also carried out in the presence of advection, i.e., non-zero *Pe*. Results are presented in Fig. 4(a) and (b) in the form of phase change front as a function of time, and temperature distributions at a given time, respectively. Two different values of *Pe* are considered in both cases. The numerical simulation is carried out using a fully implicit variable time-step method [17]. In this method, the space domain is divided into equal intervals, Δx. However, the grid size of the time domain, Δt, varies and is determined in such a way that during this time interval, the phase change front location moves a distance Δx. This ensures that the location of the phase change front always remains at a grid point. In these simulations, the space domain is divided into 1000 nodes and the timestep is calculated in an iterative fashion with a convergence error less than 0.01%. Accuracy of the numerical computation is further ensured by verifying grid independence, and good agreement with self-similarity solutions for standard problems. In light of the absence of an exact solution for the problem with advection, the numerical simulation data are used for comparison with the method developed in this work. Fig. 4 shows good agreement between the present work and the numerical simulation for each value of *Pe* considered here. The agreement is not exact because of the approximations involved in seeking an eigenvalue-based solution, and also possibly in the numerical calculations. The error is somewhat greater for the $Pe = 2000$ case than the $Pe = 500$ case, although the worst-case error is still less than 4.5%, which is reasonably low. The present work appears to slightly overpredict the growth of the phase change front compared to numerical simulations.

Since the solution derived in Section 2 is in the form of an infinite eigenfunction series, it is important to understand the number of terms needed for accurate computation. The effect of number of eigenvalues considered in the solution is presented in Fig. 5. Computed location of

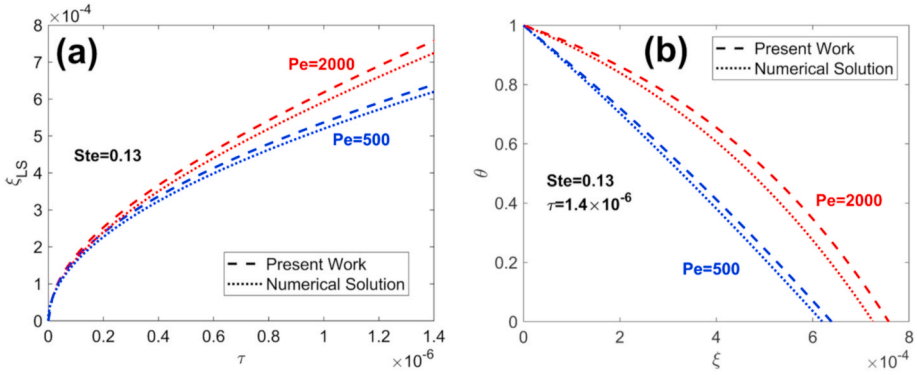

Fig. 4. Comparison of results from present work with finite-difference simulations for a one-phase problem with advection: (a) Phase change front ξ_{LS} as a function of τ; (b) Temperature distribution in liquid phases at $\tau = 1.4 \times 10^{-6}$. For both plots, $Ste = 0.13$.

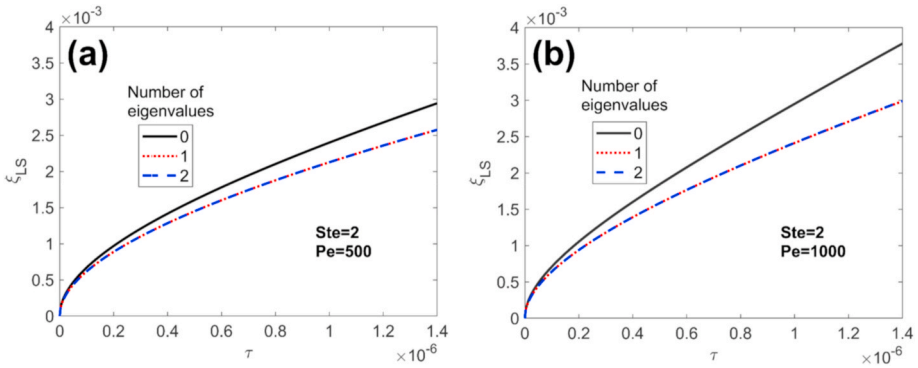

Fig. 5. Effect of the number of eigenvalues: Phase change front ξ_{LS} as a function of τ for different number of eigenvalues considered for a one-phase problem. (a) $Pe = 500$; (b) $Pe = 1000$. $Ste = 2.0$ in both cases.

the phase change front is plotted as a function of time for two different values of *Pe* in Fig. 5(a) and (b), respectively. In each case, curves are presented for zero, one and two eigenvalues in the infinite series. It is found that in both cases, considering a single eigenvalue is sufficient for convergence of results – the contribution of subsequent terms in the infinite series is negligible. This is because the transient exponential term in equation (19) decays very rapidly. Based on the definition of the eigenvalue λ_n, rapid convergence is expected unless *Pe* is small and/or ξ_{LS} is large. For most practical values of ξ_{LS} and the non-dimensional time, it is found that considering only one eigenvalue is sufficient for engineering accuracy. The accuracy in terms of percentage deviation in the predicted ξ_{LS} at $\tau = 1.4 \times 10^{-6}$ compared to a solution with 100 eigenvalues is found to be 14.2%, 0.01% and practically zero for 0, 1 and 2 eigenvalues, respectively. Based on this, for most practical applications, the infinite series in equations (19), (22) and (23) may be replaced only with the $n = 1$ term without significant loss of accuracy. The ability to use a single eigenvalue is particularly helpful for computational optimization in the present problem because the eigenvalues need to be re-computed at each time due to the changing location of phase change front.

Note that neglecting the infinite series completely is equivalent to the commonly-used quasi-stationary method, in which the temperature distribution in the liquid phase is assumed to be given by the steady-state solution of the energy conservation equation, which is valid only for small *Ste*. The infinite series may, therefore, be interpreted as a correction term for the quasi-stationary solution that helps achieve accuracy beyond that of the quasi-stationary method. The zero eigenvalue curve shown in Fig. 5 corresponds to the quasistationary solution of this problem.

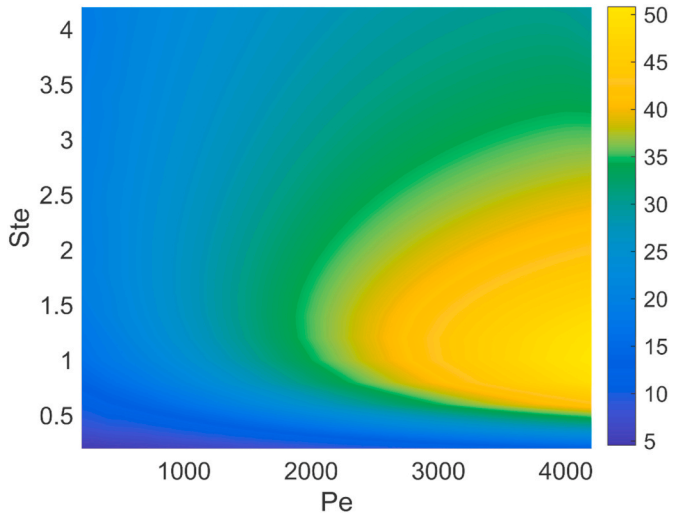

Fig. 6. Colormap showing the percentage deviation in the analytical model compared to numerical simulations for computing ξ_{LS} at $\tau = 1.4\times 10^{-6}$ in the $Ste - Pe$ parameter space for the Stefan problem.

In order to further quantify the impact of the key non-dimensional parameters on error, the deviation between the present work and numerical simulations is calculated in terms of the predicted phase change front location at $\tau = 1.4 \times 10^{-6}$. A colorplot of this percentage deviation is plotted as a function of *Pe* and *Ste* in Fig. 6. This plot shows that the error is reasonably small over a very broad range of *Pe* and *Ste*. At a fixed *Pe*, as *Ste* increases, the error reaches a maxima and then actually reduces at higher *Ste*. In comparison, the error involved in a similar phase change calculation with a quasistationary method is much larger, especially at large *Ste*. A comparison of errors associated with the present work and quasistationary method is presented as Figure S1 in Supplementary Information. Fig. 7 presents the error characteristics in the form of error curves as functions of *Ste* for two different values of *Pe* in Fig. 7(a), and as functions of *Pe* for two different values of *Ste* in Fig. 7 (b). For comparison, curves are also plotted for the quasistationary method. Fig. 7(a) shows that for small *Ste*, the error incurred in the present method is similar to the quasistationary method. However, as *Ste* increases, the error for the quasistationary method increases rapidly, whereas the error for the present work does not rise as rapidly, and actually plateaus out at large values of *Ste*. This is particularly remarkable and attractive because most approximate analytical methods for phase change heat transfer perform poorly at large *Ste*, whereas the eigenfunction based method described here retains reasonable accuracy. For both the present work as well as quasistationary method, error is greater at larger *Pe*. When comparing the two methods in terms of error as a function of *Pe*, it is found, as shown in Fig. 7(b), that at small *Ste*, both methods have similar errors as functions of *Pe*. However, at $Ste = 2.0$, the two methods behave very differently, with a much larger error for the quasistationary method compared to the present work. In this case, as *Pe* increases, the error associated with the quasistationary method increases dramatically, whereas the present method does not deteriorate as rapidly. In summary, the present method offers much greater accuracy compared to the traditional quasistationary method, and the accuracy of the method does not deteriorate dramatically at large values of *Ste* and/or *Pe*. The good performance at large *Ste* is particularly helpful in light of poor performance of other approximate analytical methods in that regime.

The effect of β, γ and θ_{in} on the deviation between the present work and numerical simulations is also investigated. By keeping other parameters constant ($Ste = 0.12$, $Pe = 1000$, $\theta_{in} = -1.5$, $\gamma = 1$), the deviation between the two in terms of ξ_{LS} at $\tau = 1.4 \times 10^{-6}$ is determined and plotted in Fig. 8(a) as a function of β between 0.3 and 1.7 that covers the expected range for most practical PCMs. Fig. 8(a) shows somewhat lower error when $\beta < 1$ compared to $\beta > 1$. However, in both cases, the error is quite small within a reasonable range of β. Similar plot

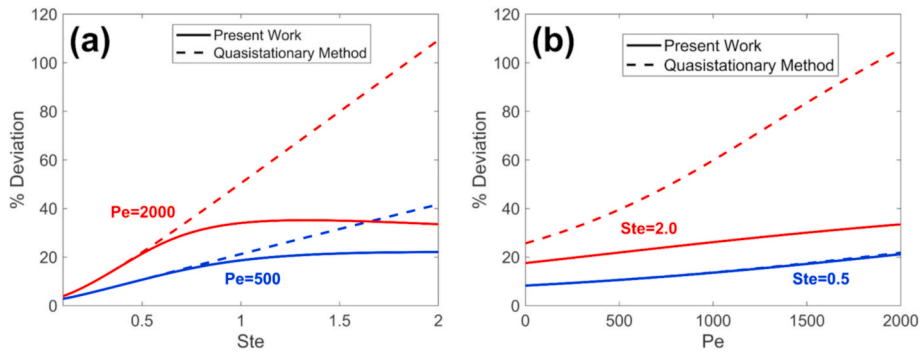

Fig. 7. Deviation in the analytical model compared to numerical simulations for computing ξ_{LS} at $\tau = 1.4 \times 10^{-6}$: (a) Percentage deviation as a function of *Ste* for a two fixed values of *Pe*; (b) Percentage deviation as a function of *Pe* for a two fixed values of *Ste*. Error curves for the quasistationary method are also shown for comparison.

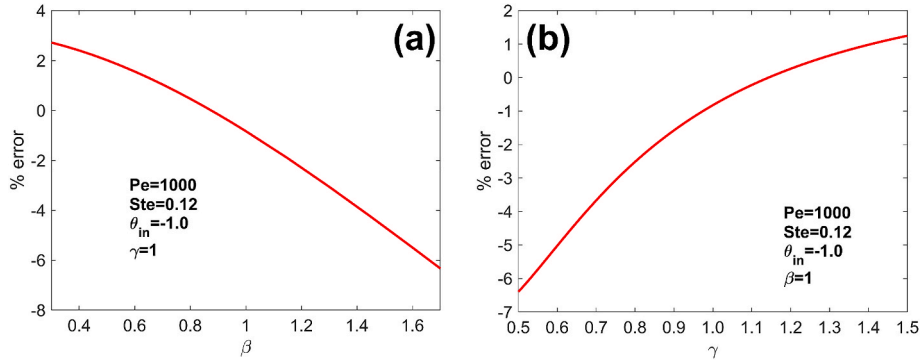

Fig. 8. Deviation in the analytical model compared to numerical simulations for computing ξ_{LS} at $\tau = 1.4 \times 10^{-6}$ as a function of (a) β with $\gamma = 1$, (b) γ with $\beta = 1$. Other parameters are $Ste = 0.12$; $Pe = 1000$; $\theta_{in} = -1.0$.

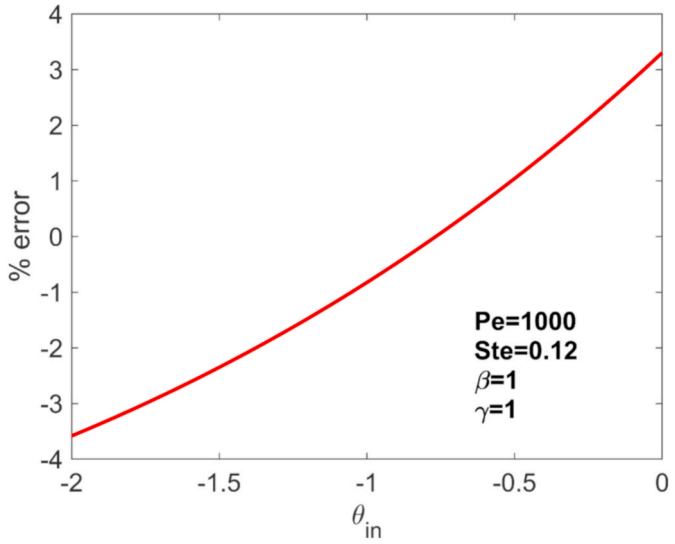

Fig. 9. Deviation in the analytical model compared to numerical simulations for computing ξ_{LS} at $\tau = 1.4 \times 10^{-6}$ as a function of θ_{in}. Other parameters are $Ste = 0.12$; $Pe = 1000$; $\beta = 1$; $\gamma = 1$.

of the deviation as a function of γ and θ_{in} are presented in Figs. 8(b) and 9, respectively. These plots are show relatively low error within a reasonable range of these parameters.

4.3. Effect of problem parameters on phase change process

The key non-dimensional parameters that govern the phase change propagation process in the presence of advection include *Pe* and *Ste*. While *Pe* represents the ratio of advection and diffusion processes, *Ste* represents the ratio of sensible to latent heat storage. The larger the value of *Ste*, the greater is the temperature difference that drives the phase change process. The initial temperature θ_{in}, and property ratios β and γ are also relevant parameters for the two-phase problem. Understanding the impact of these non-dimensional parameters on the nature of the phase change process may be helpful for the design and optimization of practical phase change energy storage and thermal management systems. Further, it is also important to understand the sensitivity of the phase change process to these parameters, some of which may not be known exactly in practical applications.

Fig. 10 presents the effect of advection represented by *Pe* on the phase change process. Plots are presented for two-phase and one-phase problems in Fig. 10(a) and (b), respectively. $Ste = 0.24$ for both cases, and for the two-phase problem, $\theta_{in} = -1.0$, $\beta = 1$, $\gamma = 1$. In each case, the phase change propagation front is plotted as a function of time. Plots show that the greater the value of *Pe*, the faster is the propagation of the phase change front. This is expected because advection through the liquid front contributes towards heat transfer from the high temperature boundary condition to the phase change front, which drives the phase change process. Zero-advection curves based on self-similarity based exact solutions are also plotted in Fig. 10(a) and (b) for comparison. It is seen that the advection curves get close to the zero-advection curve as the value of *Pe* decreases. Note that based on the definition $Pe = \frac{UL}{\alpha}$, the numerical value of *Pe* is expected to be large for practical values of the speed, since thermal diffusivity has a low numerical value for most common materials. A comparison of Fig. 10(a) and (b) shows slower

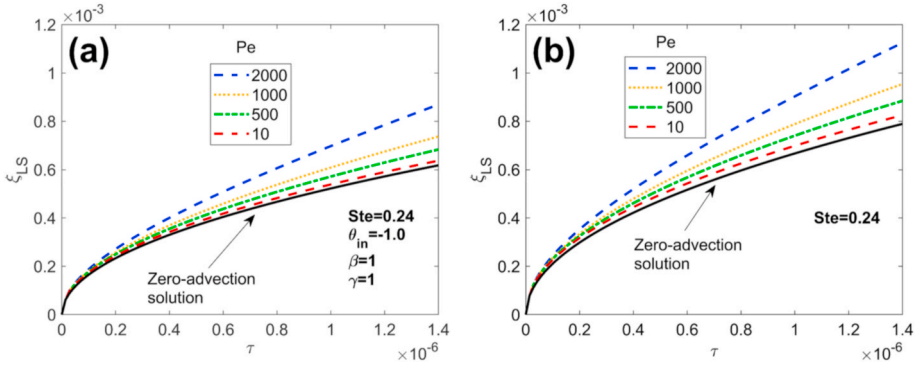

Fig. 10. Effect of *Pe* on the phase change process: Phase change front ξ_{LS} as a function of τ for different values of *Pe* for (a) two-phase problem, with $Ste = 0.24$, $\theta_{in} = -1.0$, $\beta = 1$, $\gamma = 1$; (b) one-phase problem, with $Ste = 0.24$. In both cases, the exact solution for zero-advection is also shown for comparison.

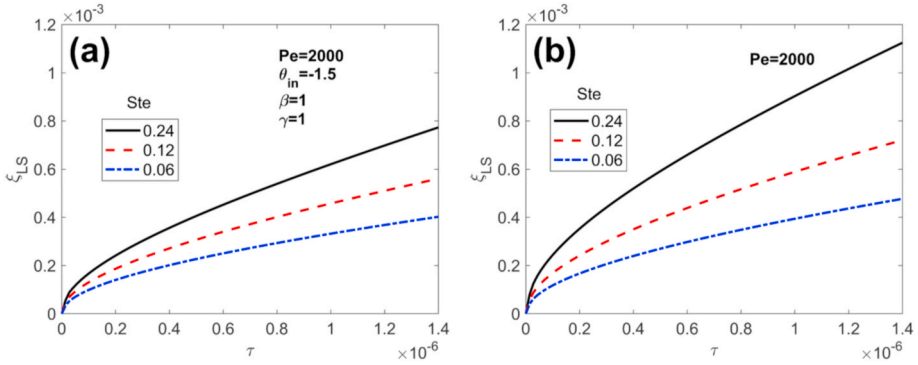

Fig. 11. Effect of *Ste* on the phase change process: Phase change front ξ_{LS} as a function of τ for different values of *Ste*for (a) two-phase problem, with $Pe = 2000$, $\theta_{in} = -1.5$, $\beta = 1$, $\gamma = 1$; (b) one-phase problem, with $Pe = 2000$.

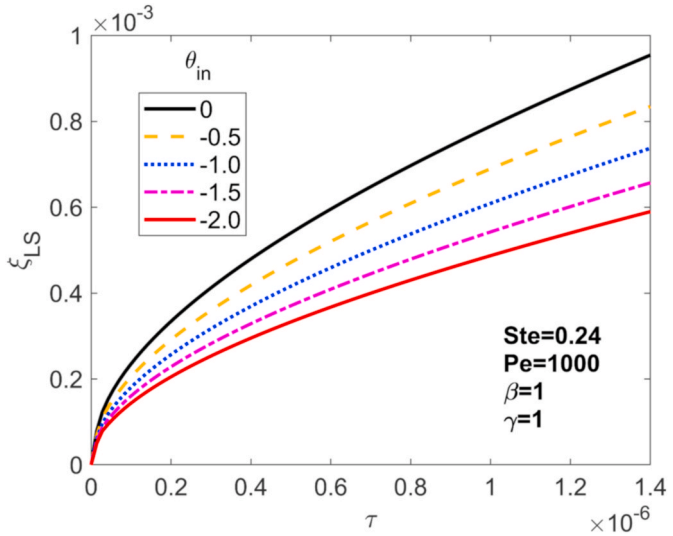

Fig. 12. Effect of initial sub-cooling, θ_{in} on the phase change process: Phase change front ξ_{LS} as a function of τ for different values of θ_{in} for a two-phase problem. Problem parameters are $Pe = 1000$, $Ste = 0.24$, $\beta = 1$, $\gamma = 1$.

phase change propagation for the two-phase problem, which is because in that case, subcooling of the solid phase must be overcome before phase change may occur.

The impact of *Ste* on the phase change process is investigated in Fig. 11. For a fixed value of $Pe = 2000$ and other non-dimensional parameters ($\theta_{in} = -1.5$, $\beta = 1$, $\gamma = 1$), Fig. 11(a) and (b) plot the propagation of the phase change front with time for three different values of *Ste* for the two-phase and one-phase problems, respectively. As expected, it is found that *Ste* plays a key role in determining the rate of phase change – the greater the value of *Ste*, the faster does phase change occur. Similar to Fig. 10, at a given value of *Ste*, phase change occurs faster for the one-phase problem where the solid is initially at the melting temperature compared to the two-phase problem, in which the solid is initially subcooled.

Fig. 12 discusses the impact of the initial sub-cooling of the solid phase on the rate of phase change propagation. A two-phase problem with $Pe = 1000$, $Ste = 0.24$, $\beta = 1$, $\gamma = 1$ is considered, and ξ_{LS} is plotted as a function of τ for different values of the initial temperature of the solid, θ_{in}. Since $T_{in} < T_m$, therefore, based on the non-dimensionalization scheme followed, the numerical value of θ_{in} is negative for two-phase problems. Fig. 12 shows that as θ_{in} decreases, i.e., the solid is more and more subcooled, the rate of phase change propagation reduces. This is along expected lines because some of the thermal energy conducted or advected through the liquid into the solid phase must be used to overcome the subcooling of the solid before phase change can occur. Therefore, the greater the degree of subcooling, the slower would be the rate at which the phase change process occurs. For reference, Fig. 12 also plots the phase change curve for $\theta_{in} = 0$, which corresponds to the one-phase problem in which the solid is initially at the melting temperature. Among all cases of θ_{in}, the rate of phase change is highest for this case, because there is no subcooling that needs to be overcome before phase change occurs.

Finally, the impact of ratios of thermal properties β and γ on the phase change process is presented in Fig. 13. β and γ represent square roots of the ratios of liquid and solid thermal diffusivity and thermal conductivity, respectively. Keeping γ constant, Fig. 13(a) plots the phase change front location as a function of time for multiple values of β. Other problem parameters are $Pe = 1000$, $Ste = 0.24$, $\theta_{in} = -1.0$. This plot

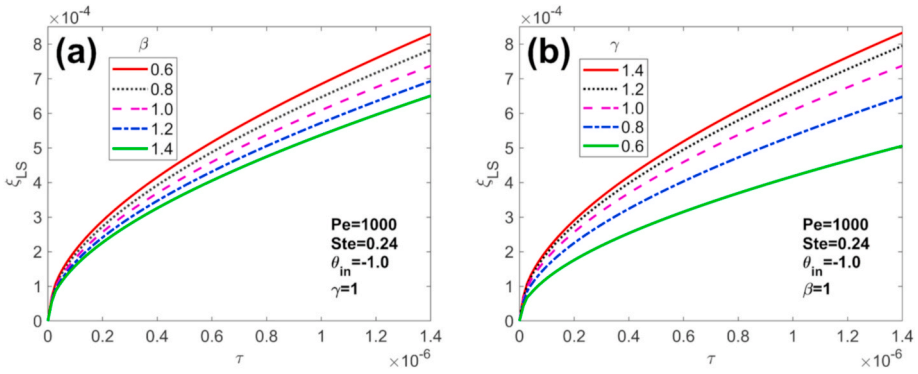

Fig. 13. Effect of non-dimensional thermal properties: Phase change front ξ_{LS} as a function of τ for (a) different values of $\beta$with fixed γ; (b) (a) different values of γ with fixed β. In both cases, $= 1000$, $Ste = 0.24$, $\theta_{in} = -1.0$.

shows faster phase change front propagation at lower values of β. This is expected because for a fixed value of the liquid thermal diffusivity, large β corresponds to lower thermal diffusivity of the solid, which impedes heat transfer into the solid the slows down the phase change process. Note that heat transfer into the solid is necessary for overcoming the subcooling of the solid in the two-phase process.

A similar analysis for the effect of γ is presented in Fig. 13(b), in which β is held constant and phase change curves are plotted for multiple values of γ. Other problem parameters are the same as in Fig. 13(a). Unlike Fig. 13(a), this plot shows that phase change occurs faster at larger values of γ. This can be understood mathematically from the $\frac{1}{\gamma^2}\left[\frac{\partial\theta_S}{\partial\xi}\right]_{\xi=\xi_{LS}}$ term in equation (14), which contributes towards determining the rate of change of the phase change front location. Note that $\left[\frac{\partial\theta_S}{\partial\xi}\right]_{\xi=\xi_{LS}}$ represents the slope of temperature distribution in the solid phase, which is clearly negative. This term reduces the rate of change of the phase change front location. Therefore, the larger the value of γ, the smaller is the negative contribution of this term, and therefore, larger is the rate of change of the phase change front location. Fig. 13(a) and (b) show that the ratios of thermal diffusivity and thermal conductivity of the two phases have opposing effects on phase change propagation. While the impact is quite uniform for β, phase change front propagation appears to be more sensitive to γ when $\gamma < 1$.

5. Conclusions

This work addresses a key gap in the phase change heat transfer literature by deriving a solution for phase change in the presence of diffusion and advection. The resulting eigenvalue-based solution can be interpreted as an improvement over the quasistationary method, in that the infinite series is a correction term resulting in reduced error. The infinite series is found to converge very rapidly, so that using a single eigenvalue is found to result in less than 0.1% error. This may be very helpful for rapid computation of the temperature distribution.

It is important to be aware of key simplifying assumptions that may limit the applicability of the theoretical model. Heat and fluid flow is assumed to be one-dimensional, and natural convection in the liquid phase is neglected. This may be a reasonable assumption for a wide variety of problems, but may not be applicable for some problems such as solidification of metal castings. Temperature-independence of thermal properties is a common assumption that is also made in the present work.

While presented in the context of heat transfer, the model presented here is equally applicable for mass transfer problems involving diffusion, advection and growth of a chemical reaction front, such as in growth of oxidation layers and SEI formation in Li-ion cells. Further, the extension of the present work for analyzing scenarios in which advection occurs in both phases, or in which the original phase is not semi-infinite can be easily carried out. Finally, the technique described here can also be used for analyzing similar phase change problems with diffusion and advection in cylindrical and spherical coordinate systems.

Declaration of competing interest

The authors declare that they have no known competing financial interests or personal relationships that could have appeared to influence the work reported in this paper.

Data availability

Data will be made available on request.

Acknowledgments

This material is based upon work supported by CAREER Award No. CBET-1554183 from the National Science Foundation.

Appendix A. Supplementary data

Supplementary data to this article can be found online at https://doi.org/10.1016/j.ijthermalsci.2021.107262.

Credit author contribution statement

M. Parhizi – Conceptualization, Methodology, Investigation, Validation, Data curation. A. Jain – Conceptualization, Methodology, Formal analysis, Investigation, Data curation, Supervision, Project administration; All authors contributed towards Writing - original draft, Review and Editing.

References

[1] R. Viskanta, Heat transfer during melting and solidification of metals, J. Heat Tran. 110 (1988) 1205–1291.
[2] X. Duan, G.F. Daterer, Heat transfer in phase change materials for thermal management of electric vehicle battery modules, Int. J. Heat Mass Tran. 53 (2010) 5176–5182.
[3] B. Zalba, J.M. Marín, L.F. Cabeza, H. Mehling, Review on thermal energy storage with phase change: materials, heat transfer analysis and applications, Appl. Therm. Eng. 23 (2003) 251–283.
[4] V.G. Gude, N. Nirmalakhandan, Desalination at low temperatures and low pressures, Desalination 244 (2009) 239–247.
[5] J.C. Slattery, Advanced Transport Phenomena, Cambridge University Press, Cambridge, MA, 1999.
[6] H.J. Ploehn, P. Ramadass, R.E. White, Solvent diffusion model for aging of lithium-ion battery cells, J. Electochem. Soc. 151 (2004) A456–A462.
[7] V. Alexiades, A.D. Solomon, Mathematical modeling of melting and freezing processes, CRC Press, 1993.
[8] A. Mori, K. Araki, Methods for analysis of moving boundary-surface problem, Int. Chem. Eng. 16 (1976) 734–744.

[9] L.I. Rubenstein, The Stefan Problem, AMS Publications, Providence, 1971.
[10] V.J. Lunardini, Heat Transfer with Freezing and Thawing, first ed., Elsevier Science, 1991.
[11] D.A. Tarzia, A Bibliography on Moving-free Boundary Problems for the Heat-Diffusion Equation. The Stefan and Related Problems,' Instituto Matematico, Ulisse Dini", Firenze, 1988.
[12] J. Stefan, Uber die Theorie des Eisbildung, insbesonder uber die Eisbildung im Polarmere, Ann. Phys. u Chem., Neue Folge 42 (1891) 269–286.
[13] F. Neumann, In Die partiellen Differentialgleichungen der mathematischen Physik, in: fifth ed., in: Weber Riemann (Ed.), Lectures Given in the 1860's, vol. 2, 1912, p. 121.
[14] M. Parhizi, A. Jain, Solution of the phase change Stefan problem with time-dependent heat flux using perturbation method, J. Heat Tran. 141 (2019), 024503: 1-5.
[15] J. Caldwell, Y.Y. Kwan, On the perturbation method for the Stefan problem with time-dependent boundary conditions, Int. J. Heat Mass Tran. 46 (2003) 1497–1501.
[16] T.R. Goodman, The heat-balance integral—further considerations and refinements, J. Heat Tran. 83 (1961) 83–85.
[17] D.W. Hahn, M.N. Özişik, Heat Conduction, Wiley, New York, 2012.
[18] V.R. Voller, C. Prakash, A fixed grid numerical modelling methodology for convection-diffusion mushy region phase-change problems, Int. J. Heat Mass Tran. 30 (8) (1987) 1709–1719.
[19] H.T. Hashemi, C.M. Sliepcevich, A numerical method for solving two-dimensional problems of heat conduction with change of phase, Chem. Eng. Prog. Symp. Ser. 63 (1967) 34–41.
[20] J.C. Álvarez-Hostos, E.A. Gutierrez-Zambrano, J.C. Salazar-Bove, E.S. Puchi-Cabrera, A.D. Bencomo, Solving heat conduction problems with phase-change under the heat source term approach and the element-free Galerkin formulation, Int. Commun. Heat Mass Tran. 108 (2019) 104321.
[21] V.R. Voller, C.R. Swaminathan, ERAL Source-based method for solidification phase change, Numer. Heat Tran., Part B Fundamentals 19 (2) (1991) 175–189.
[22] T. Xiong, L. Zheng, K.W. Shah, Nano-enhanced phase change materials (NePCMs): a review of numerical simulations, Appl. Therm. Eng. 178 (2020) 115492.
[23] G.S. Cole, Transport processes and fluid flow in solidification, in: T.J. Hugel, G. F. Bolling (Eds.), Solidification, AIME Publishing, 1969, pp. 201–274.
[24] D.L.R. Oliver, J.E. Sunderland, 'A phase change problem with temperature-dependent thermal conductivity and specific heat, Int. J. Heat Mass Tran. 30 (1987) 2657–2661.
[25] J. Crepeau, A.S. Siahpush, Solid–liquid phase change driven by internal heat generation, Compt. Rendus Mec. 340 (7) (2012) 471–476.
[26] K.N. Rai, J. Singh, A numerical study on non-Fourier heat conduction model of phase change problem with variable internal heat generation, J. Eng. Math. 129 (1) (2021) 1–16.
[27] S.I. Barry, J. Caunce, Exact and numerical solutions to a Stefan problem with two moving boundaries, Appl. Math. Model. 32 (1) (2008) 83–98.
[28] M. Grabo, E. Acar, E.Y. Kenig, Modeling and improvement of a packed bed latent heat storage filled with non-spherical encapsulated PCM-Elements, Renew. Energy 173 (2021) 1087–1097.
[29] Z. Li, C. Du, D. Ahmadi, R. Kalbasi, S. Rostami, Numerical modeling of a hybrid PCM-based wall for energy usage reduction in the warmest and coldest months, J. Therm. Anal. Calorim. 144 (2021) 1985–1998.
[30] B. Rubinsky, A. Shitzer, Analytic solutions to the heat equation involving a moving boundary with applications to the change of phase problem (the inverse Stefan problem), J. Heat Tran. 100 (2) (1978) 300.
[31] G.M.M. Reddy, M. Vynnycky, J.A. Cuminato, An efficient adaptive boundary algorithm to reconstruct Neumann boundary data in the MFS for the inverse Stefan problem, J. Comput. Appl. Math. 349 (2019) 21–40.
[32] E. Casella1, M. Giangi, An analytical and numerical study of the Stefan problem with convection by means of an enthalpy method, Math. Methods Appl. Sci. 24 (9) (2001) 623–639.
[33] M. Boukrouche, G. Łukaszewicz, The stationary Stefan problem with convection governed by a non-linear Darcy's law, Math. Methods Appl. Sci. 22 (7) (1999) 563–585.
[34] Y. Fahuak, Q. Yipin, On Stefan problem with prescribed convection, Acta Math. Sci. 14 (2) (1994) 153–166.
[35] J.R. Cannon, E. DiBenedetto, G.H. Knightly, The bidmensional stefan problem with convection: the time dependent case, Commun. Part. Differ. Equ. 8 (14) (1983) 1549–1604.
[36] N.S. Bondareva, M.A. Sheremet, Numerical investigation of the two-dimensional natural convection inside the system based on phase change material with a source of volumetric heat generation, Thermophys. Aeromechanics 25 (4) (2018) 525–537.
[37] J.M. Huang, M.J. Shelley, D.B. Stein, A stable and accurate scheme for solving the Stefan problem coupled with natural convection using the Immersed Boundary Smooth Extension method, J. Comput. Phys. 432 (2021) 110162.
[38] V. Barbu, I. Ciotir, I. Danaila, Existence and uniqueness of solution to the two-phase Stefan problem with convection, Appl. Math. Optim. (2021) 1–35, in press.
[39] J. Bollati, A.C. Briozzo, Stefan problems for the diffusion–convection equation with temperature-dependent thermal coefficients, Int. J. Non Lin. Mech. 134 (2021) 103732.
[40] K.N. Rai, J. Singh, Wavelet based numerical approach of non-classical moving boundary problem with convection effect and variable latent heat under the most generalized boundary conditions, Eur. J. Mech. B Fluid 87 (2021) 1–11.
[41] R. Dai, Q. Bian, Q. Wang, M. Zeng, Evolution of natural convection melting inside cavity heated from different sides using enthalpy based lattice Boltzmann method, Int. J. Heat Mass Tran. 121 (2018) 715–725.
[42] D. McCord, J. Crepeau, A. Siahpush, J.A.F. Brogin, Analytical solutions to the Stefan problem with internal heat generation, Appl. Therm. Eng. 103 (2016) 443–451.
[43] L. Barannyk, P. Paulus, J. Crepeau, A. Siahpush, Fourier-Bessel series model for the Stefan problem with internal heat generation in cylindrical coordinates, in: Int. Conf. Nuclear Eng., 2018. London, July 22-26.